Journal of Alloys and Compounds 523 (2012) 43–48

Contents lists available at SciVerse ScienceDirect

Journal of Alloys and Compounds

journal homepage: www.elsevier.com/locate/jallcom

Magnetocaloric effect in the ferromagnetic $GdNi_4M$ (M = Al, Si) and antiferromagnetic $NdNiAl_4$ compounds

T. Toliński[a,*], M. Falkowski[a], K. Synoradzki[a], A. Hoser[b], N. Stüßer[b]

[a] Institute of Molecular Physics, Polish Academy of Sciences, M. Smoluchowskiego 17, 60-179, Poznań, Poland
[b] Helmholtz-Zentrum, Glienicker Straße 100, D-14109, Berlin, Germany

ARTICLE INFO

Article history:
Received 7 December 2011
Received in revised form 29 January 2012
Accepted 30 January 2012
Available online 10 February 2012

PACS:
71.20.Lp
75.30.Sg
75.40.-s
61.05.fm

Keywords:
Intermetallics
Magnetically ordered materials
Heat capacity
Magnetocaloric
Magnetic measurements
Neutron diffraction

ABSTRACT

Magnetocaloric (MCE) effect has been studied in the ferromagnetic (FM) $GdNi_4Al$, $GdNi_4Si$, and the antiferromagnetic (AFM) $NdNiAl_4$ compounds. All the compounds order magnetically between 9 and 30 K. The maximum magnetic entropy change $-\Delta S_M$ is in the range of 10–16 J kg^{-1} K^{-1} for the studied RNi_4M compounds. Arrott plots suggest that the phase transition in $GdNi_4Al$ and $GdNi_4Si$ may be of a first order-type. It is ascribed to a field-induced AFM–FM transition. Neutron diffraction experiments on $NdNiAl_4$ show that its magnetic structure is not of a simple AFM-type. Additionally, the specific heat measurements for $NdNiAl_4$ reveal a change of the sign of MCE and very small values of $-\Delta S_M$ and the adiabatic temperature change ΔT_{ad}.

1. Introduction

Lanthanides-based magnetic compounds focus much attention in the search for materials having a large magnetocaloric effect (MCE). It concerns both the possible applications in the room temperature range and at low temperatures. The former provides the possibility to substitute the gas-based thermodynamic cycle of the standard refrigerators by the environment-friendly magnetization–demagnetization processes. The most widely studied and promising materials consist of the various modifications of the $Gd_5Ge_2Si_2$ compound [1], which has revealed a giant MCE (GMCE). On the other hand, the low temperature studies aim to improve the technique of the cooling in the physical investigations at the lowest temperatures or the development of the hydrogen liquefiers [2]. One of the key aspects is the order of the magnetic phase transition. A first-order transition provides the best MCE properties reported in literature. It is often accompanied by structural transformations.

This paper describes the magnetic and MCE properties in the ferromagnetic (FM) $GdNi_4Al$, $GdNi_4Si$, and the antiferromagnetic (AFM) $NdNiAl_4$ compounds. All the compounds order magnetically between 9 and 30 K. $DyNi_4Al$ is included in the studies for a verification of the sensitivity of the MCE effect to the substitution of Gd in $GdNi_4Al$ by another lanthanide ion.

It is instructive to present the MCE result for $NdNiAl_4$, which is evidently AFM as it helps to understand better the behaviour of $GdNi_4M$. In the parent compound of the $GdNi_4M$ series, i.e. $GdNi_5$, the Gd moments (7 μ_B) induce antiparallel moments of 0.16 μ_B on the Ni atoms, which can be neglected and this, in principle antiferrimagnetic compound, can be treated as a ferromagnet [3]. A similar assumption works also well for the $GdNi_4M$ compounds; however, as we show in this paper the AFM interactions can be important to explain some observations.

The $NdNiAl_4$ compound crystallizes in the $YNiAl_4$-type orthorhombic structure and is antiferromagnetic [4–6] with the Nd moments ordered along the b-axis below T_N = 9.5 K. A metamagnetic phase transition occurs for this compound at 4.4 T. The Ni atoms do not show a noticeable magnetism. For comparison, the isostructural $PrNiAl_4$ and $TbNiAl_4$ compounds reveal ordering along the a-axis [7,8], which results from the different magnetic anisotropies of the ions.

* Corresponding author. Tel.: +48 61 8695 249; fax: +48 61 8684 524.
E-mail address: tomtol@ifmpan.poznan.pl (T. Toliński).

0925-8388/$ – see front matter © 2012 Elsevier B.V. All rights reserved.
doi:10.1016/j.jallcom.2012.01.156

Table 1
The lattice parameters of the compounds discussed within the text.

Compound	Space group	a (Å)	c (Å)	Ref.
$GdNi_5$	P6/mmm	4.900	3.970	[9]
$GdNi_4Al$	P6/mmm	4.960	4.037	[10]
$GdNi_4Si$	P6/mmm	4.904	3.977	Present study
$DyNi_4Al$	P6/mmm	4.945	4.045	[10,11]
$NdNiAl_4$	Cmcm	16	8.1	Present study

The MCE properties studied within the present paper provides new observations about the phase transitions in the ferromagnetic RNi_4M (R – rare earth) and the antiferromagnetic $NdNiAl_4$ compounds and it is shown that substitutions in the parent $GdNi_5$ binary compound can improve the MCE performance.

2. Experimental

The $GdNi_4Al$, $GdNi_4Si$, $DyNi_4Al$, and $NdNiAl_4$ compounds were prepared in a polycrystalline form by induction melting of the constituent elements under an argon atmosphere.

Measurements of the magnetization curves and the magnetic susceptibility were carried out on the commercial Quantum Design Physical Property Measurement System (PPMS) equipped in the vibrating sample (VSM) option. The magnetic susceptibility has been obtained in the following modes: ZFC (zero field cooled – the sample is cooled down without a field, then the field is switched on and the measurement is carried out during heating); FC (field cooled – measurement is carried out in a magnetic field during cooling); FCH (field cooled heating – measurement is carried out in a magnetic field during heating just after the FC mode is complete).

The heat capacity data were collected by the relaxation method (two-τ model) using the same PPMS apparatus in the temperature range 2–300 K and magnetic fields up to 9 T.

Full-pattern Rietveld refinements (program FULLPROF) of our X-ray diffraction measurements have confirmed that the studied RNi_4M samples crystallize in the hexagonal $CaCu_5$-type structure. Rare earths occupy the 1a site (0,0,0) and Ni(1) is located in the 2c site (1/3, 2/3, 0). Ni(2) and the M atoms are statistically distributed over the 3g sites (1/2, 0, 1/2). The lattice parameters are collected in Table 1. For the antiferromagnetic $NdNiAl_4$ compound the neutron diffraction experiments were additionally performed at the E6 diffractometer of the Helmholtz-Centrum, Berlin. The neutron wavelength was 2.432 Å. The sample was mounted in a cryomagnet with vertical magnetic fields up to 5 T.

3. Ferromagnetic RNi_4M compounds

Gd-based intermetallic compounds are often investigated from the point of view of the magnetocaloric effect because they usually guarantee a small hysteresis of the magnetic properties. We have previously shown that both $GdNi_4Al$ and $GdNi_4Si$ exhibit similar ferromagnetic behaviour [10,12,13] with the ordering temperatures being in the range interesting for low temperature MCE applications. Figs. 1 and 2 show the temperature dependence of the magnetic susceptibility and the insets display the magnetization curves for $GdNi_4Al$ and $GdNi_4Si$, respectively. The corresponding temperatures of the ferromagnetic ordering are $T_C = 28$ K and $T_C = 25$ K if using the Arrott plots for their extraction. In Figs. 1 and 2 one can see a rather sharp drop of the magnetic susceptibility at a low magnetic field (0.01 T) both for the FC and ZFC measurements. It becomes rounded (see Fig. 1) after application of a larger magnetic field; simultaneously, the split of the FC and ZFC curves is reduced. The sharp change of $\chi(T)$ at a low field suggests that the magnetic phase transition may be of the first order-Type. Additionally, in Fig. 1 the FCH measurement is shown. The thermal hysteresis between FCH and FC is often treated as a sign of the possibility of the first order phase transition. This split also disappears in a higher magnetic field, i.e. all the FC, ZFC, and FCH curves merge in $\mu_0 H = 0.1$ T (Fig. 1).

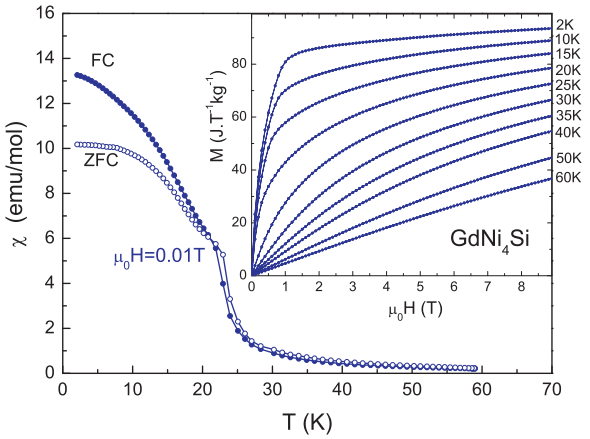

Fig. 2. Temperature dependence of the magnetic susceptibility for $GdNi_4Si$ in the ZFC and FC mode. Inset: magnetization curves – only selected temperatures are displayed for a better legibility.

Such a transition seems to be supported by the Arrott plot representation of the magnetization curves, i.e. by plotting M^2 vs. $\mu_0 H/M$. The corresponding plot is included in Fig. 3 for $GdNi_4Al$ and it is similar for $GdNi_4Si$ (not shown). Following the Banerjee criterion [14] a first order transition is suspected if the slope of the Arrott plot is negative. The inset of Fig. 3 reveals that the slope change occurs for small magnetic field values. It coincides with the sharp change of the magnetic susceptibility measured at a low field. Recapping, it seems possible that the magnetic phase transition is of the first order in $GdNi_4Al$ and $GdNi_4Si$; however, it should be borne in mind

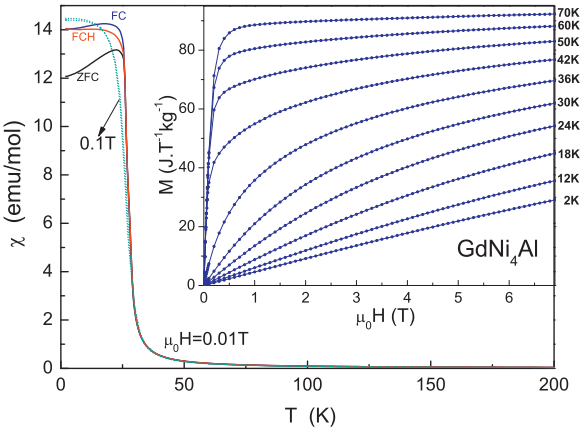

Fig. 1. Temperature dependence of the magnetic susceptibility for $GdNi_4Al$ measured in the ZFC, FC, and FCH modes (see the text). Inset: magnetization curves – only selected temperatures are displayed for a better legibility.

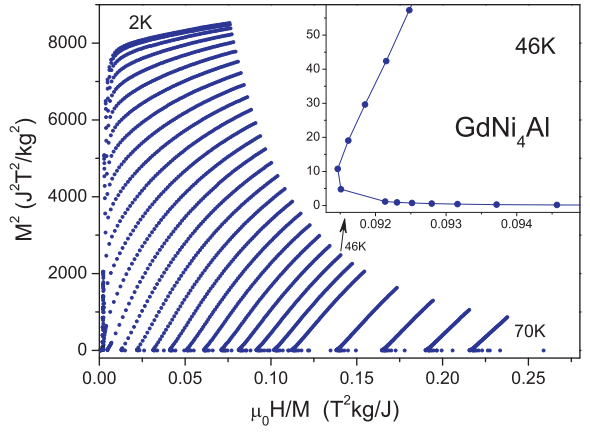

Fig. 3. Arrott plots M^2 vs. $\mu_0 H/M$ for the $GdNi_4Al$ compound. Similar behaviour is observed for $GdNi_4Si$ (not shown). Inset: Enlargement of the data region for $T = 46$ K and low values of M^2 (the axes titles are identical with the main figure).

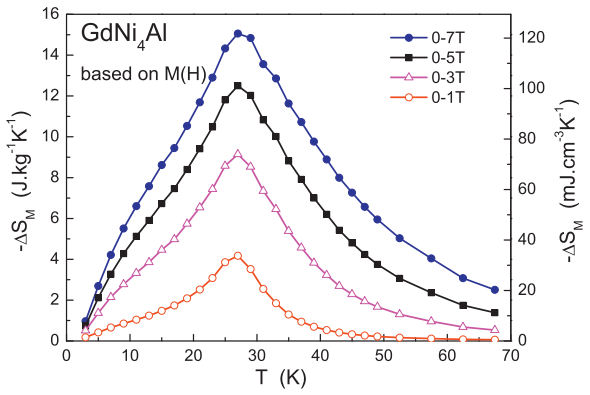

Fig. 4. Magnetic entropy change $-\Delta S_M$ determined based on the magnetization curves $M(H)$ and Eq. (1) for $GdNi_4Al$.

that for the parent isostructural binary compound, $GdNi_5$, a second order phase transition at 31 K has been reported [9,15]. The observation of the features of the first order-type transition only at a low magnetic field may be due to another reason, e.g. a slight amount of impurities, however they are not detectable in our X-ray diffraction measurements. Moreover, in the low temperature neutron diffraction studies of the isostructural $DyNi_4Al$ compound [11] we have not observed any structural transition. Hence, the most plausible explanation of the Arrott plots appears after recalling that a small magnetic moment exists on the Ni atoms, which is antiparallel to the rare earth moment. It was observed for the parent compound $GdNi_5$ [3] but we found it also for ternary RNi_4M compounds by electronic structure calculations and X-ray magnetic circular dichroism (XMCD) measurements [16,13,17]. Therefore, the slope change of the Arrott plots can be ascribed to a field-induced first order type AFM-FM transition. Similar behaviour of the M^2 ($\mu_0 H/M$) curves has been observed by Shen et al. [18]. Hence, already a small magnetic field switches the system to the FM state (Figs. 1 and 3) and the change from the ferromagnetic to the paramagnetic (PM) state proceeds via a second order transition.

Next we determine the MCE effect in the studied compounds. The Maxwell's thermodynamic relation [2,19,20]:

$$\Delta S_M(T) \approx \frac{\mu_0}{\delta T}\left[\int_0^{H_{max}} M(T+\delta T, H)dH - \int_0^{H_{max}} M(T,H)dH\right] \quad (1)$$

yields the isothermal magnetic entropy change by simple integration of the magnetization curves $M(H)$. δT is the temperature difference between two isotherms. The temperature dependence of $-\Delta S_M$ for $GdNi_4Al$ and $GdNi_4Si$ is illustrated in Figs. 4 and 5 both in the J kg^{-1} K^{-1} and mJ cm^{-3} K^{-1} units and in magnetic fields used

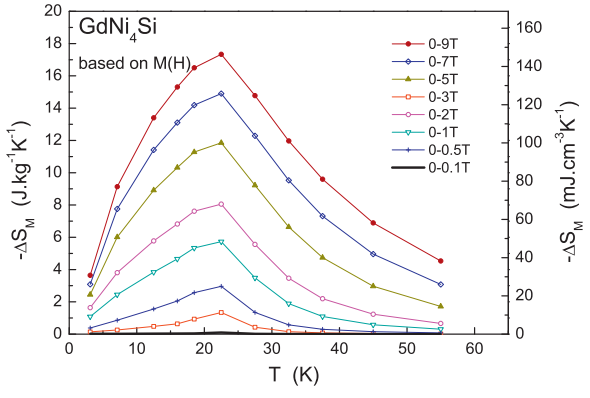

Fig. 5. Magnetic entropy change $-\Delta S_M$ determined based on the magnetization curves $M(H)$ and Eq. (1) for $GdNi_4Si$.

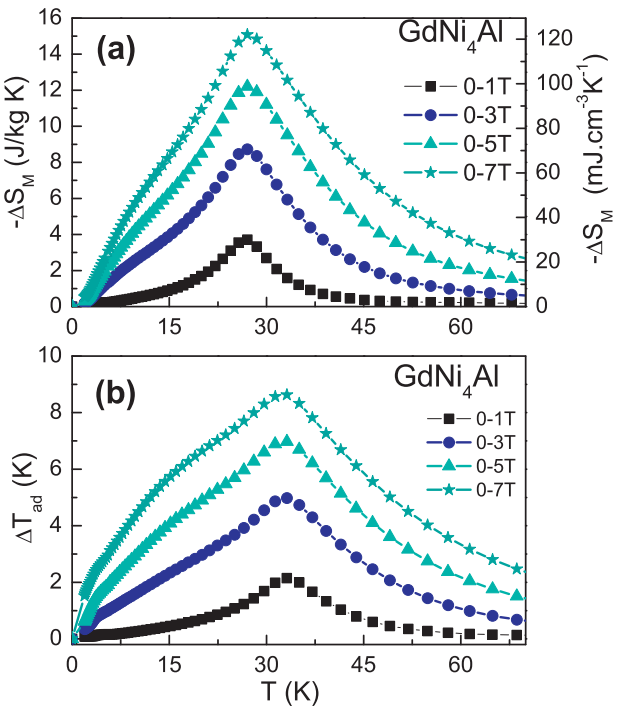

Fig. 6. $GdNi_4Al$: the magnetic entropy change $-\Delta S_M$ (a) and the adiabatic temperature change ΔT_{ad} (b) determined based on the heat capacity (Eq. (2)) for various magnetic field changes.

usually in literature for comparisons of the MCE between various materials. Both the Gd-based compounds exhibit similar values of the isothermal entropy change.

Further, we intend to confirm the reliability of MCE obtained from the magnetization isotherms by measurements of the specific heat. Apart from $-\Delta S_M$ it enables additionally the derivation of the adiabatic temperature change ΔT_{ad}. The isomagnetic entropy is calculated directly from the specific heat data by the integration:

$$S(T)_H = \int_0^T \frac{C_p(T)_H}{T} dT \quad (2)$$

Figs. 6 and 7 present the temperature dependence of $-\Delta S_M$ and ΔT_{ad} for the $GdNi_4Al$ and $GdNi_4Si$ compounds. The values obtained for $-\Delta S_M$ are in good agreement with the calculation based on the isothermal magnetizations (Figs. 4 and 5). The peaks of these dependences are relatively narrow comparing with the isostructural $GdNi_5$ compound [9,21]. The low temperature hump results probably from the gradual occupation of the crystal electric field levels.

Table 2 gathers the main MCE parameters for the compounds studied and for the parent $GdNi_5$. It is evident that a partial substitution of Ni with Al or Si slightly improves the magnetocaloric performance of the $GdNi_5$ compound. To verify the effect of the rare earth type, the MCE of the $DyNi_4Al$ compound has been measured and is presented in Fig. 8 and included in Table 2. It provides similar values of the characteristic parameters as $GdNi_4Al$ and $GdNi_4Si$ but the ordering temperature is significantly reduced [10,11].

4. Antiferromagnetic $NdNiAl_4$ compound

It has previously been shown that $NdNiAl_4$ is antiferromagnetic [4–7] with the Nd moments ordered along the b-axis below $T_N = 9.5$ K. A metamagnetic phase transition occurs for this compound at 4.4 T. Fig. 9 presents the neutron diffraction pattern measured at 20 K, i.e. in the paramagnetic state and refined with the program FULLPROF. The low angle parts of this pattern

Table 2
The maximum magnetic entropy change $-\Delta S_M$, the adiabatic temperature change ΔT_{ad} and the relative cooling power parameters for selected intermetallic compounds. Where possible, similar parameters for the literature examples have been estimated. RCP/ΔH does not change much with the magnetic field, hence only values for single fields are provided.

Compound	Tord (K)	$-\Delta$SM (J kg^{-1} K^{-1})	ΔTad (K)	RCP(S) (J/cm^3)	RCP(T) (K^2)	RCP(S)/ΔH (mJ/cm^3 k Oe)	RCP(T)/ΔH (K^2/k Oe)
GdNi5 [9]	34						
5T		10.5		~2.5			
7T		12.5		~3			
GdNi4Al	28						
5T		12.2	7	2.73	263		
7T		15.1	8.6	3.84	376	55	5.37
GdNi4Si	25						
5T		12.6	8.4	2.77	210		
7T		15.7	10.5	3.81	290	54.4	4.15
DyNi4Al	11						
5T		11	8	2.22	182		
7T		12.9	9.9	3.42	251	48.8	3.58
NdNiAl4	9.5						
6T		1.7/−3.3	1.74/−1.4	0.013/−0.019	11.5/−10	0.22/−0.32	0.19/−0.16
TbNiAl4 [22]							
4T	27; 35	−5.1	−3.3	~0.08	~40	~2	~1
DyCo3B2 [23]							
5T	22	13.3	10	5.35	299		
7T		15.4	11.9	5.44	408	76.4	5.80
TbCo3B2 [24]							
7T	28	10.3	8.6				
GdCo3B2 [25]							
7T	54	11.6	6.4				

measured at 2 K and zero magnetic field as well as in 2 K and $\mu_0 H = 5$ T are shifted upwards in Fig. 9 and the arrows indicate the magnetic reflections. The location of the magnetic reflections suggests that the magnetic structure is not of a simple antiferromagnetic type. A propagation vector $k = (0.076, 0.352, 0.478)$ has been proposed [5]. Our rough analysis provides a close result, $k = (0.175, 0.295, 0.434)$; however, like in Ref. [5] we find that the weak magnetic intensities cannot be well refined for the powdered samples and studies on single crystalline samples are necessary. It seems also that the magnetic contribution due to the Ni atoms should be included in the analysis.

The top pattern in Fig. 9 presents the neutron diffraction data collected in 2 K and $\mu_0 H = 5$ T, which is a magnetic field larger than that for the metamagnetic transition. One can observe a disappearance of some magnetic peaks, growth of the other and the appearance of a few new peaks. This behaviour cannot be quantitatively interpreted due to the difficulty to exclude fully the rotation of the powder grains towards the direction of the magnetic field.

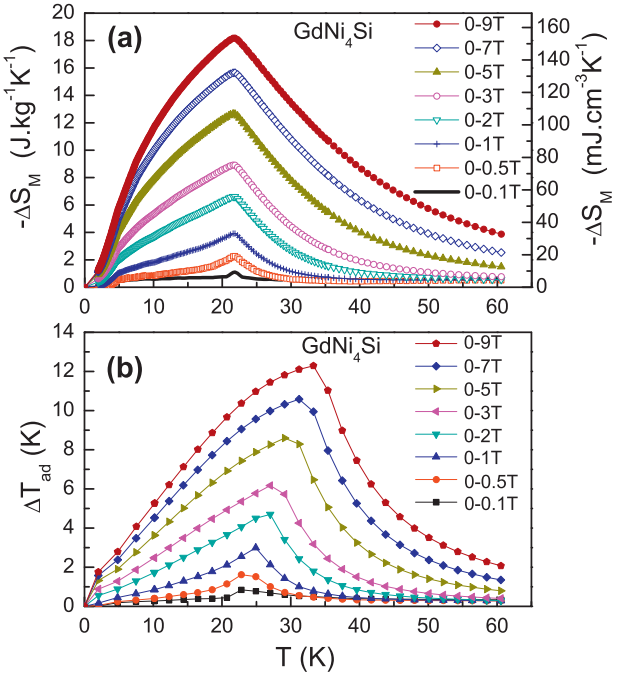

Fig. 7. $GdNi_4Si$: the magnetic entropy change $-\Delta S_M$ (a) and the adiabatic temperature change ΔT_{ad} (b) determined based on the heat capacity (Eq. (2)) for various magnetic field changes.

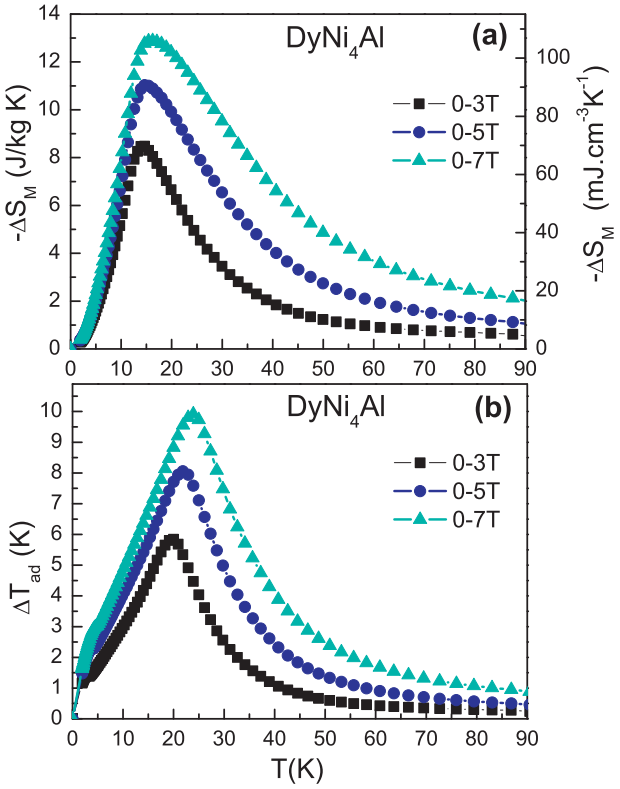

Fig. 8. $DyNi_4Al$: the magnetic entropy change $-\Delta S_M$ (a) and the adiabatic temperature change ΔT_{ad} (b) determined based on the heat capacity (Eq. (2)) for various magnetic field changes.

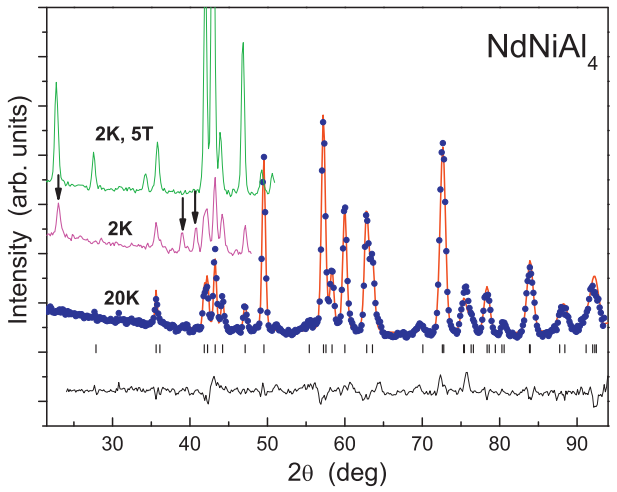

Fig. 9. Neutron diffraction pattern of $NdNiAl_4$ at 20 K fitted with FULLPROF. The low angle pattern shifted upwards represents the measurement at 2 K (below the AFM transition) with the magnetic reflections indicated by arrows. The top pattern corresponds to 2 K and $\mu_0 H = 5$ T. The ticks at the bottom denote the structural reflections. The bottom curve corresponds to the difference between the calculated and the experimental pattern measured at 20 K.

It is only evident that not all the non-structural peaks disappear, hence the sample does not fully switch to the ferromagnetic state at $\mu_0 H = 5$ T.

The influence of the magnetic field on the temperature dependence of the specific heat confirms the AFM-type of order. It is visible in Fig. 10 that the peak decreases and shifts toward lower temperatures with the increase of the magnetic field value. A magnetic field exceeding the value of the metamagnetic transition leads to a change of the temperature dependence of the specific heat below the ordering temperature. It is visible in Fig. 10 that for $\mu_0 H = 6$ T a hump grows at about 5 K, which may be due to an additional change of the magnetic ordering type.

The MCE effect (Fig. 11) is characterized by small values of the magnetic entropy change and the adiabatic temperature change. These parameters reveal a peculiar behaviour, namely they change the sign, which may stem from the complicated magnetic structure. Similar behaviour has been observed in Dy_3Co [26] but in that case the sign change has been dumped in magnetic fields larger than 2 T. For $TbNiAl_4$ an inverse MCE was found by Li et al. [22] but it was not accompanied by the sign change in spite of the proofed presence of two magnetic phase transitions [8,22]. von Ranke et al.

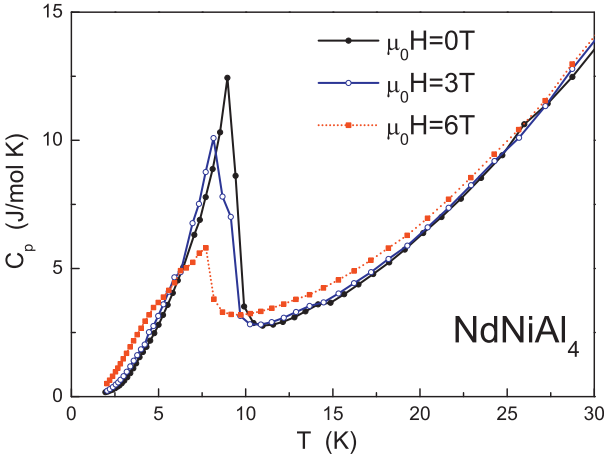

Fig. 10. Temperature dependence of the specific heat for $NdNiAl_4$ in selected magnetic fields.

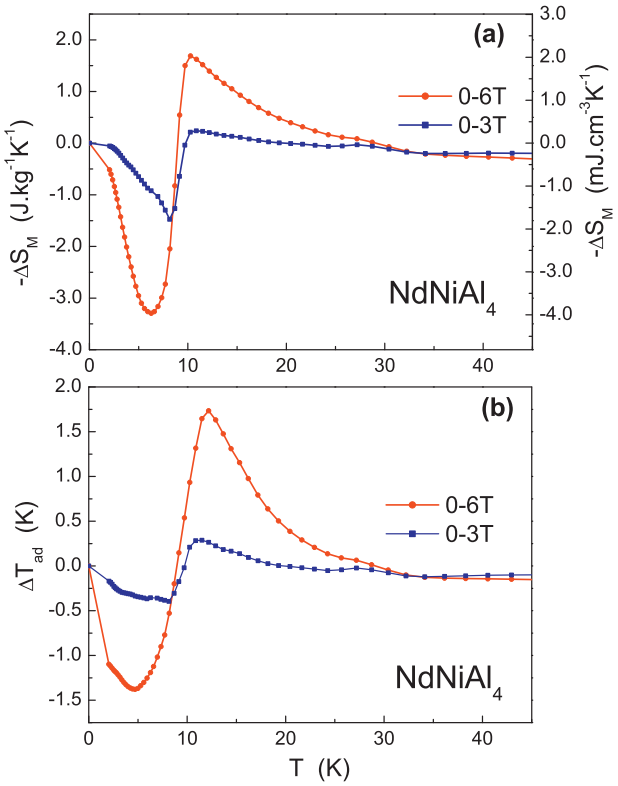

Fig. 11. $NdNiAl_4$: the magnetic entropy change $-\Delta S_M$ (a) and the adiabatic temperature change ΔT_{ad} (b) determined based on the heat capacity (Eq. (2)) for various magnetic field changes.

[27,28] found a similar anomalous behaviour in the case of the binary compounds $PrNi_5$ and $DyAl_2$ and explained the sign change theoretically using Hamiltonian containing the crystal electric field (CEF) and the exchange interactions. For the former compound the effect is due to the CEF levels crossing and for the latter one it is due to the first order phase transition in the easy magnetic direction.

A quite different temperature dependences of MCE for $GdNi_4M$ corroborates that the AFM interactions are not predominant for those compounds.

All the compounds studied and the comparative literature results are collected in Table 2 including several parameters commonly used for the estimation of the practical applicability of the MCE material. The first one is the relative cooling power (RCP) [20], which is a product of the maximum values of ΔT_{ad} or ΔS_M and the full width at half maximum of $\Delta T_{ad}(T)$ or $\Delta S_M(T)$ curves. It is also useful to use the normalized magnitudes, i.e. $RCP(S)/\Delta H$ and $RCP(T)/\Delta H$; in this case we use kOe as the units of the magnetic field to facilitate a comparison with the literature data.

5. Conclusions

It has been shown that the compounds $GdNi_4Al$, $GdNi_4Si$ and $DyNi_4Al$ exhibit moderate values of the maximum magnetic entropy change $-\Delta S_M$ and the adiabatic temperature change ΔT_{ad} if compared with intermetallic compounds of similar magnetic ordering temperatures. Arrott plots allow for a possibility of a first order phase transition between the paramagnetic and ferromagnetic state but it is at variance with the previous evidence for the parent $GdNi_5$ compound. However, it can be reasonable explained by a field-induced AFM-FM transition considering the antiparallel alignment of the small Ni magnetic moments in respect the rare earth moments.

The antiferromagnetic $NdNiAl_4$ compound shows a negligible magnetocaloric effect; however, it attracts attention due to a peculiar change of the sign of MCE in the neighbourhood of the magnetic ordering temperature. Our neutron diffraction studies confirm that the magnetic order is not in the form of a simple antiparallel spins' alignment and it seems that the inclusion of the Ni magnetism may be necessary to explain the magnetic structure of $NdNiAl_4$.

Acknowledgment

This work was supported by the funds of the National Science Centre as a research project no. N N507 219540 in years 2011–2013.

References

[1] V.K. Pecharsky, K.A. Gschneidner Jr., Phys. Rev. Lett. 78 (1997) 4494.
[2] K.A. Gschneidner Jr., V.K. Pecharsky, A.O. Tsokol, Rep. Prog. Phys. 68 (2005) 1479.
[3] Handbook on the Physics and Chemistry of Rare Earths, vol. 32. In: Karl, A.G, LeRoy, E., Lander, G.H. (Eds.).
[4] T. Mizushima, Y. Isikawa, T. Yasuda, T. Kuwai, J. Sakurai, J. Phys. Soc. Jpn. 68 (1999) 637.
[5] T. Mizushima, Y. Isikawa, J. Sakurai, K. Mori, T. Fukuhara, K. Maezawa, J. Schweizer, E. Ressouche, Physica B 194 (1994) 225.
[6] K. Nishimura, K. Mori, S. Teraoka, W.D. Hutchison, D.H. Chaplin, S. Ohya, T. Ohtsubo, S. Muto, T. Shinozuka, Hyperfine Interact. 158 (2004) 199.
[7] K. Nishimura, T. Yasukawa, K. Mori, Y. Isikawa, W.D. Hutchison, D.H. Chaplin, Jpn. J. Appl. Phys. 42 (2003) 5565.
[8] W.D. Hutchison, D.J. Goossens, K. Nishimura, K. Mori, Y. Isikawa, A.J. Studer, J. Magn. Magn. Mater. 301 (2006) 352.
[9] N. Bucur, E. Burzo, R. Tetean, J. Optoelectron. Adv. Mater. 10 (2008) 801.
[10] T. Toliński, Mod. Phys. Lett. B 21 (2007) 431.
[11] T. Toliński, W. Schäfer, A. Kowalczyk, B. Andrzejewski, A. Hoser, A. Szlaferek, J. Alloys Compd. 385 (2004) 28.
[12] T. Toliński, V. Ivanov, A. Kowalczyk, Mater. Sci. 24 (2006) 789.
[13] A. Kowalczyk, A. Szajek, M. Falkowski, G. Chełkowska, J. Magn. Magn. Mater. 305 (2006) 348.
[14] S.K. Banerjee, Phys. Lett. 12 (1964) 16.
[15] A.M. Mulders, P.C.M. Gubbens, C.T. Kaiser, A. Amato, F.N. Gygax, A. Schenck, P. Dalmas De Réotier, A. Yaouanc, K.H.J. Buschow, F. Kayzel, A.A. Menovsky, Hyperfine Interact. 133 (2001) 197.
[16] T. Toliński, M. Pugaczowa-Michalska, G. Chełkowska, A. Szlaferek, A. Kowalczyk, Phys. Status Sol. B 231 (2002) 446.
[17] T. Toliński, J.C. Cezar, H. Wende, A. Kowalczyk, K. Baberschke, Acta Phys. Pol. A 115 (2009) 129.
[18] J. Shen, Z.X. Xu, H. Zhang, X.Q. Zheng, J.F. Wu, F.X. Hu, J.R. Sun, B.G. Shen, J. Magn. Magn. Mater. 323 (2011) 2949.
[19] V.K. Pecharsky, K.A Gschneidner Jr., J. Appl. Phys. 86 (1999) 565.
[20] A.M. Tishin, Y.I. Spichkin, in: J.M.D. Coey, D.R. Tilley, D.R. Vij (Eds.), The Magnetocaloric Effect and its Applications, Series in Condensed Matter Physics, IOP, 2003.
[21] E. Burzo, I.G. Pop, D.N. Kozlenko, J. Optoelectron. Adv. Mater. 12 (2010) 1105.
[22] L. Li, K. Nishimura, W.D. Hutchison, J. Phys.: Conf. Ser. 150 (2009) 042113.
[23] T. Toliński, M. Falkowski, A. Kowalczyk, K. Synoradzki, Solid State Sci. 13 (2011) 1865.
[24] L. Li, D. Huo, H. Igawa, K. Nishimura, J. Alloys Compd. 509 (2011) 1796.
[25] L. Li, K. Nishimura, H. Igawa, D. Huo, J. Alloys Compd. 509 (2011) 4198.
[26] J. Shen, J.L. Zhao, F.X. Hu, G.H. Rao, G.Y. Liu, J.F. Wu, Y.X. Li, J.R. Sun, B.G. Shen, Appl. Phys. A 99 (2010) 853.
[27] P.J. von Ranke, V.K. Pecharsky, K.A. Gschneidner, B.J. Korte, Phys. Rev. B 58 (1998) 14436.
[28] P.J. von Ranke, I.G. de Oliveira, A.P. Guimarães, X.A. da Silva, Phys. Rev. B 61 (2000) 447.